3 Multiscale *In Silico* Modeling of Cartilage Injuries

Rami K. Korhonen, Atte S. A. Eskelinen, Gustavo A. Orozco, Amir Esrafilian, Cristina Florea, and Petri Tanska

Abstract

Injurious loading of the joint can be accompanied by articular cartilage damage and trigger inflammation. However, it is not well-known which mechanism controls further cartilage degradation, ultimately leading to post-traumatic osteoarthritis. For personalized prognostics, there should also be a method that can predict tissue alterations following joint and cartilage injury. This chapter gives an overview of experimental and computational methods to characterize and predict cartilage degradation following joint injury. Two mechanisms for cartilage degradation are proposed. In (1) biomechanically driven cartilage degradation, it is assumed that excessive levels of strain or stress of the fibrillar or non-fibrillar matrix lead to proteoglycan loss or collagen damage and degradation. In (2) biochemically driven cartilage degradation, it is assumed that diffusion of inflammatory cytokines leads to degradation of the extracellular matrix. When implementing these two mechanisms in a computational *in silico* modeling workflow, supplemented by *in vitro* and *in vivo* experiments, it is shown that biomechanically driven cartilage degradation is concentrated on the damage environment, while inflammation via synovial fluid affects all free cartilage surfaces. It is also proposed how the presented *in silico* modeling methodology may be used in the future for personalized prognostics and treatment planning of patients with a joint injury.

Keywords

Cartilage · Injury · Modeling · Loading · Degradation

3.1 Introduction

Abnormal loading of the joint is one of the most common risk factors of osteoarthritis (OA) (Fig. 3.1). Injurious loading of the joint may cause damage to articular cartilage or other joint tissues, possibly resulting in excessive forces or deformations in specific regions of the joint surfaces. Subsequently, these processes may lead to articular cartilage degeneration and post-traumatic OA [2, 3]. Joint injury can also trigger inflammation and increase expression of aggrecanases (such as a dis-

R. K. Korhonen (✉) · A. S. A. Eskelinen
A. Esrafilian · C. Florea · P. Tanska
Department of Technical Physics, University of Eastern Finland, Kuopio, Finland
e-mail: rami.korhonen@uef.fi

G. A. Orozco
Department of Technical Physics, University of Eastern Finland, Kuopio, Finland

Department of Biomedical Engineering, Lund University, Lund, Sweden

B. K. Connizzo et al. (eds.), *Electromechanobiology of Cartilage and Osteoarthritis*, Advances in Experimental Medicine and Biology 1402, https://doi.org/10.1007/978-3-031-25588-5_3

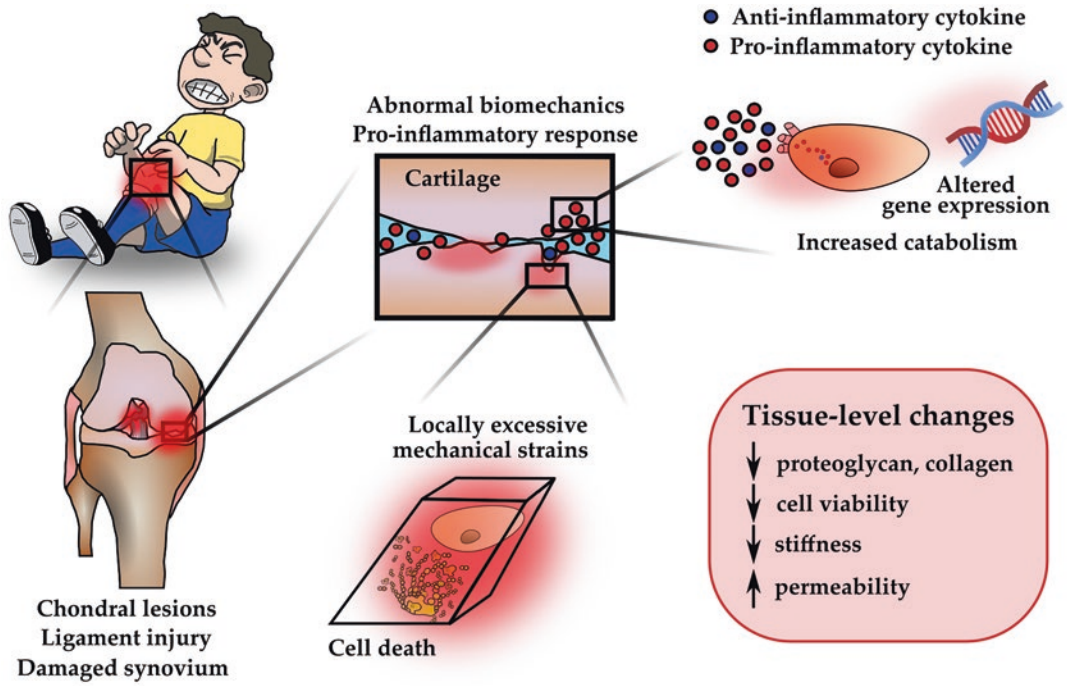

Fig. 3.1 Overview of cartilage degradation mechanisms triggered by a joint injury. An injury may result in lesions on articular cartilage surfaces, ligament tearing, and synovium damage. Together, these damages promote a catabolic joint environment encompassing abnormal biomechanical loading patterns and pro-inflammatory cytokines diffusing into cartilage. The former could lead to locally elevated mechanical strains or stresses, suggested to lead to cell death, collagen network damage and PG loss. It can also lead to release of reactive oxygen species, and cell death due to necrosis (acute) and apoptosis (persisting abnormal loading). The latter mechanism upregulates catabolic and suppresses anabolic gene expression in chondrocytes. Ultimately, injured cartilage exhibits loss of PG and collagen contents, lower cell viability, smaller stiffness, and higher permeability compared to healthy cartilage [15, 26, 46]

integrin and metalloproteinase with thrombospondin motifs, ADAMTS-4,5) [35] and collagenases (such as matrix metalloproteinase, MMP-1,13) [58], degrading the extracellular matrix of cartilage, particularly collagen and proteoglycans (PGs). However, the relationship between biomechanically and biochemically driven deterioration of injured cartilage and progression of post-traumatic OA is not well known. Moreover, prevention and personalized treatment of OA is possible only if the disease progression can be predicted. In this chapter, we provide evidence for both degeneration mechanisms through multiscale *in vitro* and *in vivo* experiments and *in silico* finite element (FE) modeling. We also showcase *in silico* modeling approaches for personalized prediction of OA progression. Generally, for more detailed understanding, we refer to specific publications in each sub-chapter.

3.2 Experiments to Study Tissue Alterations Following Cartilage Injury

3.2.1 General

In order to understand biomechanically and biochemically driven mechanisms leading to cartilage degradation in detail, *in vitro* experiments have often been conducted [8, 23]. In contrast to *in vivo* animal model experiments or clinical studies, in *in vitro* measurement setups one can fully control both biomechanical and biochemical environments of the samples.

3.2.2 Setup

A typical *in vitro* measurement setup to study tissue alterations following cartilage injury has been described in Fig. 3.2. Here, articular cartilage plugs were subjected to injurious loading under unconfined compression (50–65% strain amplitude, 100–400%/s strain rate), often producing small cracks on the cartilage surface [9, 11, 21, 38, 40, 53]. This was followed by cyclic (dynamic) loading (10–30% strain amplitude, 0.5–1 Hz loading frequency, haversine waveform) and interleukin (IL)-1-challenge (1 ng/ml) for up to 24 days, both separately and combined. For the cyclic loading, 1 h loading periods with 3–10 h resting periods were applied [9, 23, 38].

3.2.3 Analysis of Structure and Composition

There are several methods to analyze alterations in cartilage structure and composition following injury. Biochemical methods have often been used to analyze glycosaminoglycan and collagen contents of the samples (dimethylmethylene blue and hydroxyproline assays, respectively [24]). Polarized light microscopy has been used to determine changes in the collagen fibril network, namely collagen fibril orientation. Fourier transform infrared imaging has been performed to quantify the spatial collagen content in cartilage, while digital densitometry analysis of Safranin-O-stained sections is suitable for evaluation of

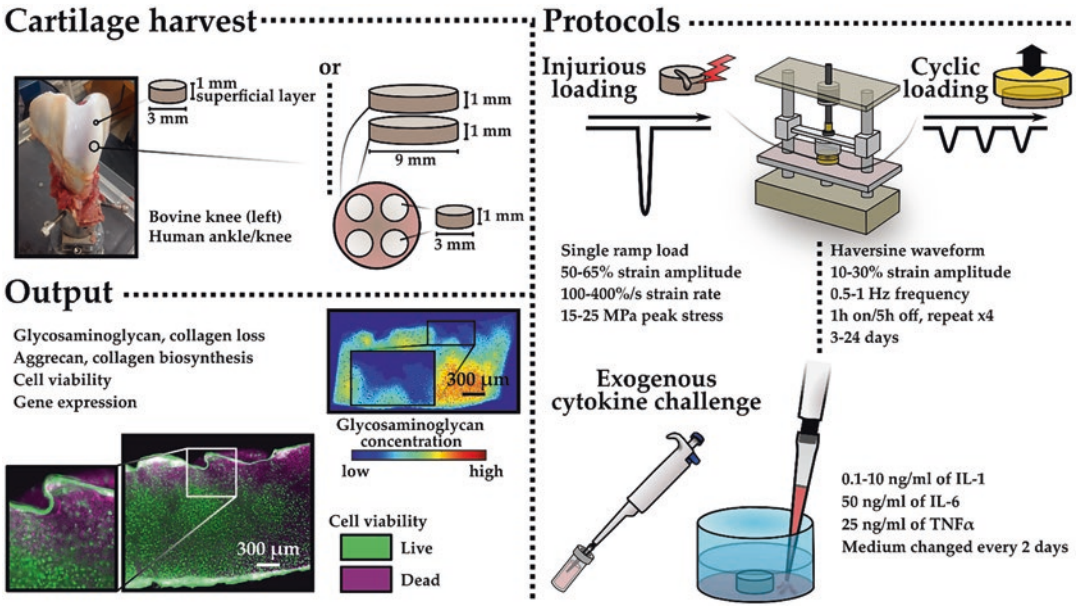

Fig. 3.2 Experimental tissue explant models of post-traumatic osteoarthritis. Cylindrical articular cartilage plugs (thickness 1 mm, diameter 3 mm) have typically been harvested from knee and ankle joints of calves and humans *post mortem*. Two controlled biomechanical loading protocols have widely been used in the *in vitro* models. The first is single injurious compressive loading in unconfined compression, leading into formation of cartilage cracks in the superficial zone. The second is cyclic (dynamic) loading mimicking daily walking, exhibiting physiological strain amplitudes and loading frequencies. To induce biochemical degradation and inflammation, exogenous administration of interleukin (IL)-1, IL-6, and/or tumor necrosis factor α (TNFα) has been used. After subjecting cartilage plugs to biomechanical loading, their PG and collagen contents and depth-wise distributions, collagen network architecture, aggrecan and collagen biosynthesis rates, cell viability, and gene expression, focusing on genes such as aggrecan and IL-1, can be analyzed [8, 9, 23, 25, 38]

the spatial PG content of the tissue. For more details, see for instance [27, 36].

3.2.4 Biological Analysis

Cell viability assays (fluorescent staining) have been used to analyze the percentage of dead cells. Real-time quantitative reverse transcription polymerase chain reaction (RT-qPCR) is a technique for investigation of gene expression in cartilage, targeting factors such as aggrecan and IL-1 [23]. On the other hand, aggrecan and collagen biosynthesis rates can be analyzed by ^{35}S-sulfate and ^{3}H-proline incorporation [45].

3.3 *In Silico* Models for Understanding Mechanisms Leading to Cartilage Degeneration

3.3.1 General

There are several constitutive material models in the literature that can characterize cartilage mechanics in different loading scenarios. Briefly, traditional poroelastic and biphasic models can distinguish between solid and fluid phases [32, 48]. When combined with anisotropic properties of the solid matrix, these models can also characterize tension–compression nonlinearity and high fluid pressurization under rapid loading conditions. Later developed fibril-reinforced poroelastic and poroviscoelastic models are able to separate the fibrillar network from the non-fibrillar matrix, and can even consider swelling of cartilage due to fixed charge density (FCD) of PGs [20, 60]. In the latter model, the total stress is given by

$$\begin{aligned}\boldsymbol{\sigma}_{\text{tot}} &= \boldsymbol{\sigma}_{\text{f}} + \boldsymbol{\sigma}_{nf} - p\mathbf{I} - T_{\text{c}}\mathbf{I} \\ &= \boldsymbol{\sigma}_{\text{f}} + \boldsymbol{\sigma}_{nf} - \Delta\pi\mathbf{I} - \mu^{\text{f}}\mathbf{I} - T_{\text{c}}\mathbf{I},\end{aligned} \tag{3.1}$$

where $\boldsymbol{\sigma}_{\text{tot}}$ is the total stress tensor, $\boldsymbol{\sigma}_{\text{f}}$ and $\boldsymbol{\sigma}_{\text{nf}}$ are the stress tensors of the fibrillar and non-fibrillar matrices, respectively, p and $\Delta\pi$ are the hydrostatic and swelling pressures, respectively, $\mathbf{I}$ is the unit tensor, μ^{f} is the chemical potential of water, and T_{c} is the chemical expansion stress. In this equation, $\boldsymbol{\sigma}_{\text{f}}$ is directly affected by the collagen volume fraction.

These highly nonlinear material models have been implemented using finite element (FE) analysis and recently applied to generate adaptive algorithms for prediction of tissue alterations due to abnormal biomechanical or biochemical environment of knee joint, cartilage, and chondrocytes [11, 17, 31, 55]. In these models, it is first assumed that the amount of a certain constituent of the tissue (particularly collagen and PGs, or FCD of PGs, or their biomechanical properties) can change over time depending on the local mechanical (stress or strain) or biochemical (amount of inflammatory cytokines) environment. A brief overview of biomechanically and biochemically driven cartilage degradation mechanisms is given in the following.

3.3.2 Theory

Part I — Biomechanically driven degradation: Biomechanically driven degradation models of cartilage first assume that overloading (stress or strain) can lead to cell death, altered tissue properties and OA [31, 47, 49]. In this approach, excessive shear or deviatoric strains of over 30% have been suggested to lead to cell death and FCD loss or non-fibrillar matrix softening, while excessive collagen fibril strains (>8%) or maximum principal stresses (>7 MPa) have been suggested to lead to collagen fibril damage and softening. The former affects directly $\Delta\pi$ and T_{c} in Eq. (3.1) and reduces swelling pressure in the tissue or softens the tissue by reducing $\boldsymbol{\sigma}_{\text{nf}}$. The latter mechanism reduces $\boldsymbol{\sigma}_{\text{f}}$ in the same equation. See more detailed mechanisms and implementation from [16, 31, 38].

In the degradation and damage algorithms, collagen fibrils can also adapt to the changing mechanical environment and bend toward maximum principal strain directions [55], simulating collagen fibril reorientation in OA. In addition,

PGs can be released directly through the tissue surface through fluid expulsion, particularly through a lesion surface where the collagen network is damaged [38, 57].

Part II — Diffusion-based biochemical degradation: In this model, the inflammatory cytokines are assumed to regulate the behavior of chondrocytes and subsequently the cartilage constituent biosynthesis and degradation [17]. The cytokines bind to corresponding receptors on the cell surface. This triggers signaling cascades within the cell which results in increased expression of aggrecanases (such as ADAMTS-4,5) and collagenases (such as MMP-1,13) which can then act in the pericellular and extracellular matrices [28, 35, 58]. Furthermore, there are tissue inhibitors of metalloproteinases (TIMPs), which inhibit the activity of ADAMTS and MMPs [35]. However, the activity of TIMPs either remains unchanged or is down-regulated by the cytokines [54]. Ultimately, when the degrading factors outweigh the matrix biosynthesis and repair, this biochemical process leads to accelerated loss of aggrecan and/or collagen.

These biochemical processes have been implemented in mechanobiological models by using reaction–diffusion partial differential equations [11, 17], which can be written as:

$$\frac{\partial C_i}{\partial t} = D_i \nabla^2 C_i \pm R_i, \tag{3.2}$$

where C_i is concentration of the constituent i (*e.g.,* chondrocyte, aggrecan, collagen, cytokine), D_i is the effective diffusivity of chemical species i, and R_i is the corresponding source–sink term, which describes the rate of generation/repair or degradation/apoptosis/consumption of individual species. Aggrecan and collagen concentration can then be linked with FCD and collagen volume fraction in Eq. (3.1), affecting directly $\Delta\pi$ and T_c or $\boldsymbol{\sigma}_f$, respectively.

In Fig. 3.3, see an example of implementation of these two degradation mechanisms in a mechanobiological model and how the model has shown to produce results comparable to experimental findings.

3.4 From *In Vitro* to *In Vivo*

3.4.1 General

In silico modeling of cartilage lesions *in vivo* includes several multiscale steps. First, clinical imaging is needed to generate the model geometry. For loading input, motion capture is needed and supplemented by musculoskeletal (MS) modeling. *In vitro* data and validated soft tissue models can then be implemented to capture biomechanically and biochemically driven degradation mechanisms of cartilage. Finally, the FE model is generated and simulated based on the input information, and the predictions are compared with literature or personalized imaging data. To get a better idea of the workflow, an example is given below (see also Fig. 3.4).

3.4.2 *In Vivo* Experiments

In a study by [37], magnetic resonance imaging (MRI) and motion analysis were conducted for subjects with anterior cruciate ligament (ACL) injury and reconstruction. Changes in $T_{1\rho}$ and T_2 relaxation times and kinematics of the subjects' knees were followed for 3 years post-surgery. $T_{1\rho}$ is generally assumed to relate with PG content, while T_2 has often been associated with collagen orientation of cartilage [41, 52]. Cone-beam computed tomography (CBCT) has also been used to image cartilage injuries [18, 43]. It can provide better resolution than MRI but has not shown capabilities for specific evaluation of cartilage structure and composition.

3.4.3 *In Vivo* FE Analysis

MRI and motion capture data at the 1-year follow-up time point were used to generate computational MS-FE models of knees [37]. Cartilage was modeled similarly as in the *in vitro* model, including biomechanically (excessive shear strains) and biochemically (diffusion of IL-1) driven degradation mechanisms. Simulation results of FCD loss

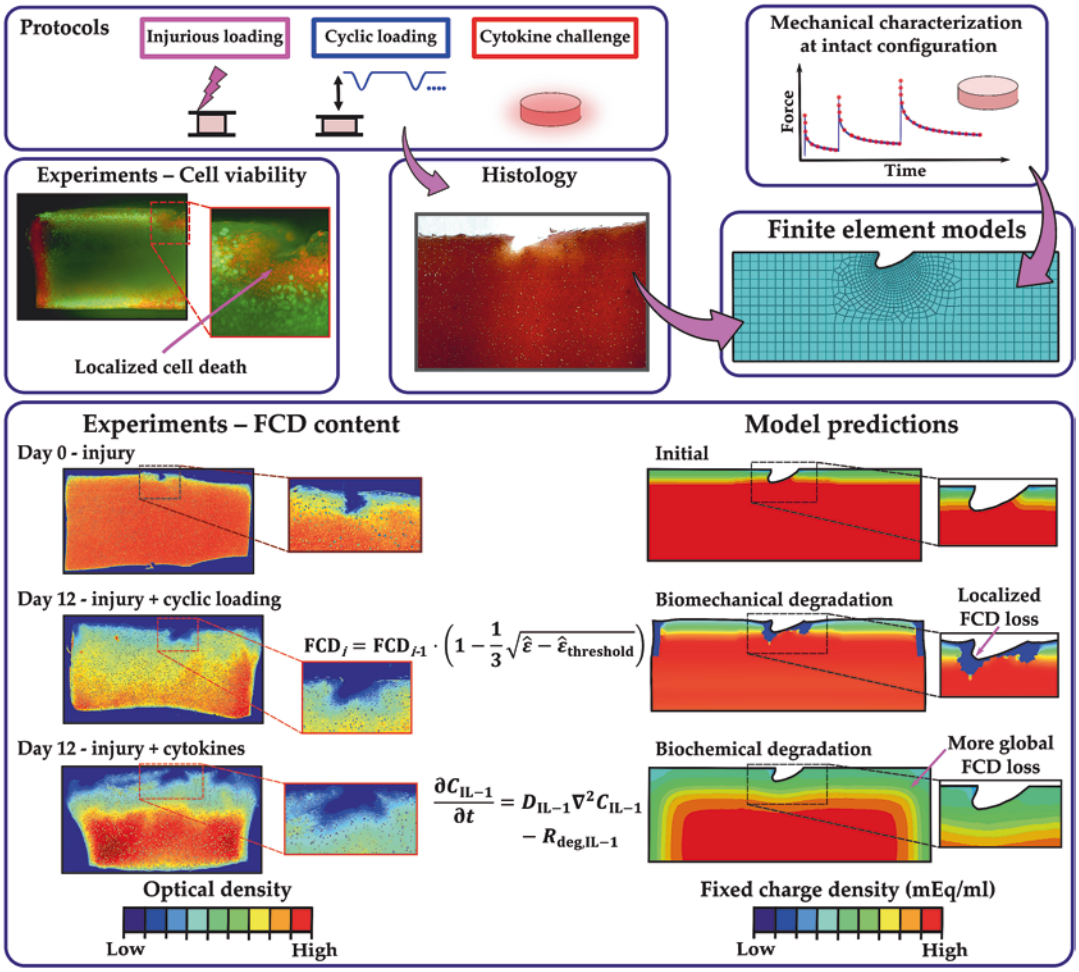

Fig. 3.3 Tissue-level *in vitro* modeling of cartilage injuries. In these examples, injurious loading experiments were simulated by an adaptive fibril-reinforced poroelastic finite element model [11, 38, 60]. Two cartilage degradation mechanisms were implemented. Biomechanically driven degradation assumed that shear strains over a threshold of 32–50% induce apoptosis and fixed charge density (FCD) loss. Biochemically driven degradation simulated diffusion of pro-inflammatory cytokine interleukin (IL)-1 (1 ng/ml) into cartilage and subsequent FCD loss. Simulated and experimental FCD losses were compared [11, 38]. (Material from: Orozco et al. [38])

were compared with changes in $T_{1\rho}$ and T_2 times during the follow-up. Similarly, *in vivo* CBCT imaging has been used to generate FE models of knees for evaluation of altered biomechanics related to cartilage injuries [34].

3.4.4 Summary from *In Vitro* and *In Vivo* Studies

Based on these selected experimental and computational studies, *in vitro* and *in vivo* results showed local FCD loss around cartilage lesions when the biomechanically driven cartilage degradation was applied. On the other hand, IL-1 diffusion via synovial fluid and subsequent FCD loss were more global and observed on the free cartilage surfaces [10, 11, 37, 38]. Therefore, it was suggested that biomechanically and biochemically driven cartilage degradation mechanisms occur simultaneously in post-traumatic OA, but they affect cartilage structure and composition differently in a location-specific manner. These two mechanisms may also have a different

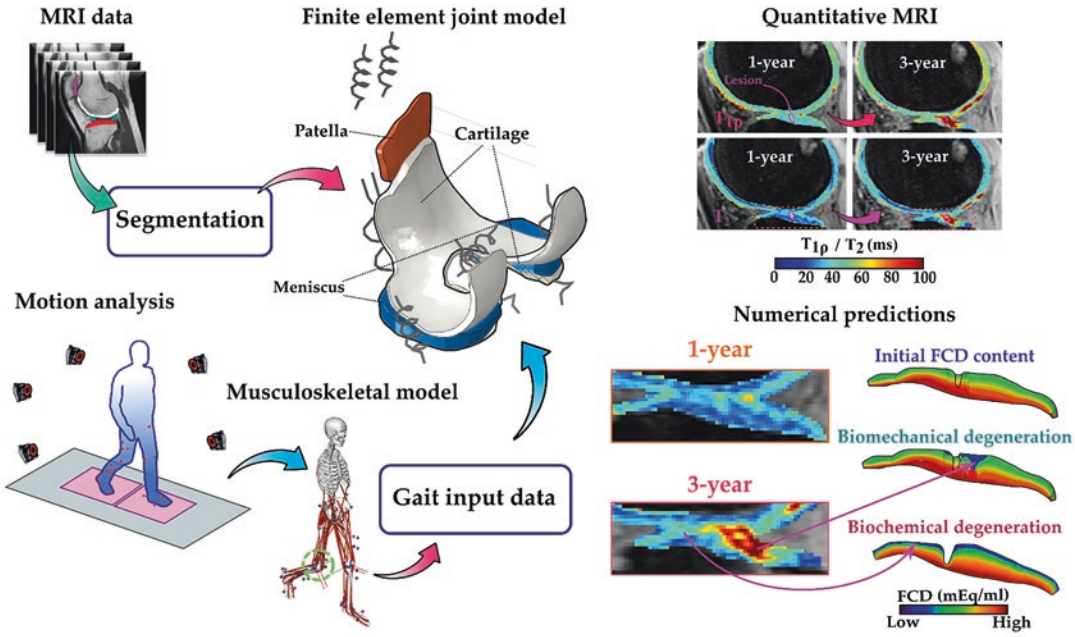

Fig. 3.4 Multiscale *in vivo* modeling of cartilage injuries. Based on *in vitro* data, validated soft tissue models and degradation mechanisms, loading scenarios, and clinical imaging, an MS-FE model was developed [37]. As can be seen on the bottom-right, biomechanically and biochemically driven degradation mechanisms predicted different locations for fixed charge density (FCD) loss (very localized *vs.* more global, respectively). These results suggest that altered biomechanics regulates tissue composition around the cartilage injury while pro-inflammatory cytokines affect all surfaces in contact with synovial fluid. (Material from: Orozco et al. [37, 39])

time-dependent response since the concentrations of cytokines vary greatly between the early acute phase after injury compared to possible later chronic phase. The introduced model could be used to estimate the effect of biomechanical and biochemical interventions on the subsequent cartilage degradation.

3.5 Toward a Clinical Assessment Tool to Aid Decision Making

Modeling workflows presented in this chapter do not yet provide any aid for clinicians to support their decision making. For this reason, all the steps in model generation and simulation should become fast and reliable. For this task, all modeling steps, including generation of the model geometry and mesh, implementation of loading and material properties, and simulation, should be automatic or at the very least semi-automatic.

Incorporating the aforementioned and complex material models requires a well-structured and precise FE mesh to be able to correctly implement different tissue constituents (*e.g.*, collagen fibril orientation and density, and fluid fraction), and also to successfully converge the FE analysis. In addition, the numerical convergence of an FE model that includes several contact-pairs, complex geometries and loading conditions, and especially large deformations of highly nonlinear materials, depends heavily on the mesh quality. Therefore, there have been attempts to develop rapid state-of-the-art MS-FE modeling and simulation pipelines, potentially feasible for clinical applications to investigate joint- and tissue-level knee mechanics in different functional activities. One of those approaches is an atlas-based FE modeling toolbox [30] along with an electromyography (EMG)-assisted, muscle force-driven MS-FE analysis workflow [12]. In this approach, based on certain anatomical

dimensions of the joint, the existing template model is scaled to match the corresponding dimensions of an individual patient. This process provides a personalized model geometry and mesh and takes only a few minutes, underlining the potential clinical applicability. The generated model is then supplemented by muscle forces, joint contact forces, and moments, as well as automatic implementation of the material properties of the soft tissues. To showcase the usability of the pipeline to estimate joint cartilage stresses and strains, indicative of tissue health and degradation, examples of simulation results of daily activities and rehabilitation exercises are given in Fig. 3.5. For more details, see Refs. [12, 13].

When supplementing this pipeline with adaptive modeling of cartilage health and degradation, as shown in previous sections, one can design personalized daily activity or rehabilitation protocols to avoid further cartilage degradation and progression of osteoarthritis.

3.6 Future Plans

In addition to the aforementioned mechanisms of cartilage degradation, high shear strains near chondral lesions may also lead to necrosis [51] and apoptosis via abrupt and excessive deformation of cell membrane and increased levels of reactive oxygen species (ROS) [5, 29]. Evidence suggests that these cell death mechanisms also result ultimately in PG loss via release of damage-associated molecular patterns and aggrecanases, ROS-amplified oxidative stress, and inflammatory response [1, 22, 29]. In the light of the cell-level experimental findings, it is now widely accepted that elevated pro-inflammatory factors and subsequent catabolic cell responses play a key role in the pathogenesis of post-traumatic OA [61]. There is also evidence that the pericellular matrix acts as a transducer of biochemical and biomechanical signals for chondrocytes, regulating their metabolic activity in response to environmental signals [6, 7, 14]. Alterations in the pericellular matrix properties and cell–matrix interactions may also contribute to OA initiation and progression. Currently, next-generation *in silico* models are under development considering both cell death and ROS-activity, as well as other introduced mechanisms in this chapter, and these models could help better understand post-traumatic OA progression and possible recovery of the PG content in temporally changing mechanobiological environments [19, 33].

No consensus exists whether there is an association between symptomatic and radiographic OA [50, 59]. Since cartilage does not have nerves, pain is often not associated with the structural progression of OA until at later disease stages, but is rather related to other tissues, such as bone and ligaments, or to inflammation. However, mechanisms of pain are still an unexplored topic in the field of computational modeling, and they should be known before implementing them in any *in silico* modeling framework.

While the development and validation of high-fidelity and highly detailed predictive models is essential to improve the understanding of mechanisms leading to OA, the development of artificial intelligence (AI)-based models is needed for fast prediction. There are sophisticated AI-based methods for diagnosis of OA [4, 44, 56] and real-time simulation of joint contact forces [42]. Fed by personalized information, such methods could be applied for fast and even real-time prediction of OA progression and simulation of the effects of interventions, pushing towards a more low-fidelity and simpler, but as accurate as the high-fidelity, tool for clinical use. When supplemented with rapid X-ray imaging, wearables, and 2D video imaging rather than MRI and extensive 3D motion capture, the future *in silico* models could provide a means for an out-of-lab setting where clinical environment would not be needed to obtain prognosis and enable monitoring. This could best enable informed patient participation in self-management of lifestyle and physical activity interventions, which is a crucial factor in prevention or delay of the progression of OA and even more importantly in improving the patients' quality of life.

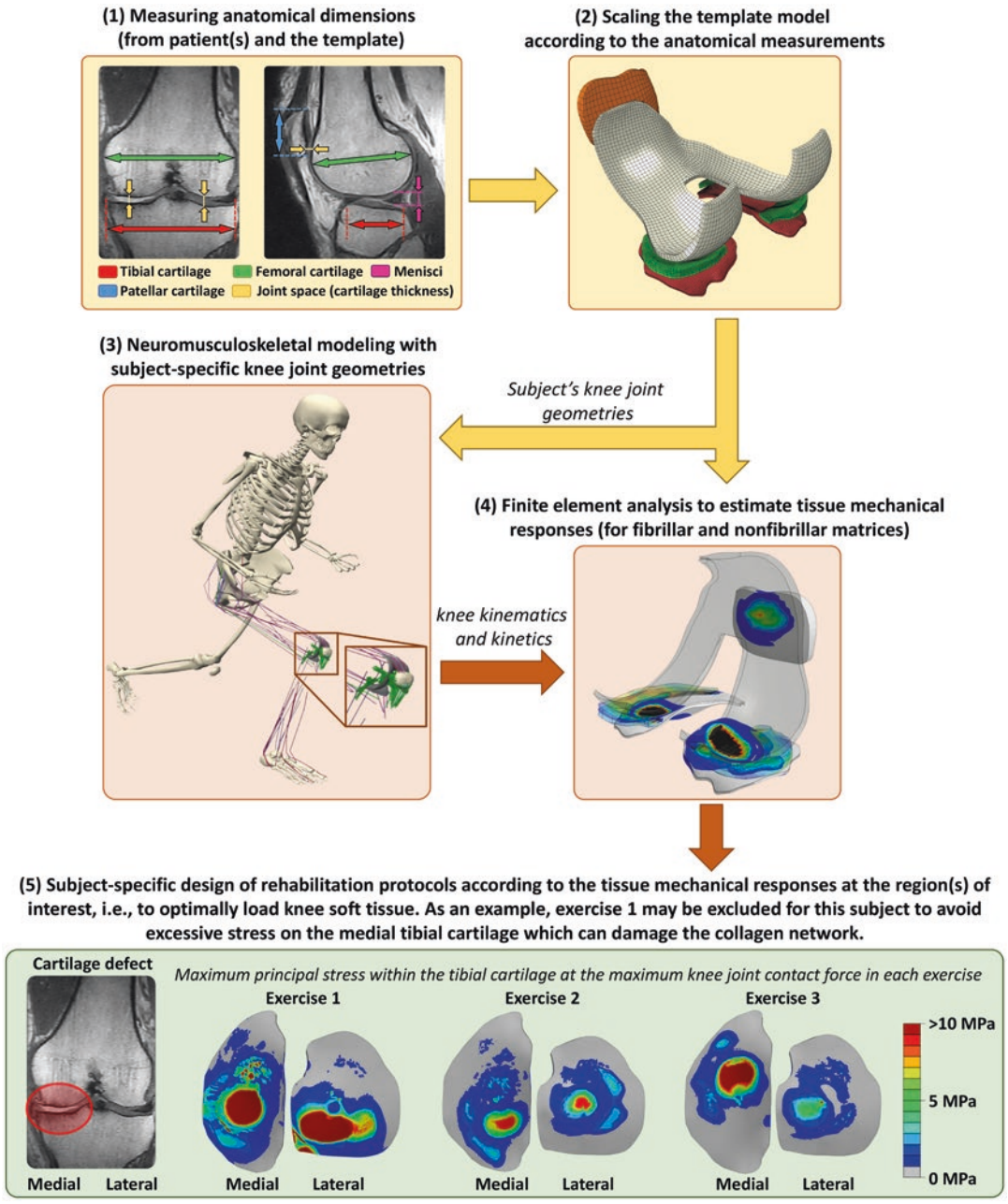

Fig. 3.5 Atlas-based rapid MS-FE modeling, toward a clinical assessment tool to aid decision making. (1): Anatomical dimensions are measured from subject's and the template's medical images, such as MRI. (2): The template FE model (*i.e.*, meshed geometries) are anisotropically scaled according to the anatomical dimensions. Note that the template FE model contains the fibril-reinforced poroviscoelastic material model, contact pairs, *etc.*, enabling rapid generation of the subject's FE model. (3): Neuromusculoskeletal modeling is used to estimate subject's kinematics, muscle forces, and joint contact forces to provide the FE model with subject-specific inputs. The MS model can incorporate subject's muscle activation patterns (*i.e.*, measured by electromyography) and subject's knee joint geometries (obtained from the scaled FE model) within the analysis. (4): Using joint kinematics and kinetics from neuromusculoskeletal modeling, FE analysis is used to estimate tissue-level joint mechanics for fibrillar (collagen network) and non-fibrillar (PGs) matrices. (5): The estimated tissue mechanics in different rehabilitation exercises can be used to assist clinicians with decision making, *i.e.*, designing subject-specific rehabilitation protocols to avoid excessive loading and accelerated degradation of the joint cartilage regions with defects. (For more details, see Refs. [12, 13])

References

1. Ansari MY, Ahmad N, Haqqi TM (2020) Oxidative stress and inflammation in osteoarthritis pathogenesis: role of polyphenols. Biomed Pharmacother 129:110452. https://doi.org/10.1016/j.biopha.2020.110452
2. Arokoski JPA, Jurvelin JS, Väätäinen U, Helminen HJ (2000) Normal and pathological adaptations of articular cartilage to joint loading. Scand J Med Sci Sports 10:186–198. https://doi.org/10.1034/j.1600-0838.2000.010004186.x
3. Bader DL, Salter DM, Chowdhury TT (2011) Biomechanical influence of cartilage homeostasis in health and disease. Arthritis 979032:1–16. https://doi.org/10.1155/2011/979032
4. Brahim A, Jennane R, Riad R et al (2019) A decision support tool for early detection of knee OsteoArthritis using X-ray imaging and machine learning: data from the OsteoArthritis initiative. Comput Med Imaging Graph 73:11–18. https://doi.org/10.1016/j.compmedimag.2019.01.007
5. Brouillette MJ, Ramakrishnan PS, Wagner VM et al (2014) Strain-dependent oxidant release in articular cartilage originates from mitochondria. Biomech Model Mechanobiol 13:565–572. https://doi.org/10.1007/s10237-013-0518-8
6. Chery DR, Han B, Li Q et al (2020) Early changes in cartilage pericellular matrix micromechanobiology portend the onset of post-traumatic osteoarthritis. Acta Biomater 111:267–278. https://doi.org/10.1016/j.actbio.2020.05.005
7. Chery DR, Han B, Zhou Y et al (2021) Decorin regulates cartilage pericellular matrix micromechanobiology. Matrix Biol 96:1–17. https://doi.org/10.1016/j.matbio.2020.11.002
8. DiMicco M, Patwari P, Siparsky P et al (2004) Mechanisms and kinetics of glycosaminoglycan release following in vitro cartilage injury. Arthritis Rheum 50:840–848. https://doi.org/10.1002/art.20101
9. Eskelinen A, Florea C, Tanska P et al (2022) Cyclic loading regime considered beneficial does not protect injured and interleukin-1-inflamed cartilage from post-traumatic osteoarthritis. J Biomech 141:111181. https://doi.org/10.1016/j.jbiomech.2022.111181
10. Eskelinen ASA, Mononen ME, Venäläinen MS et al (2019) Maximum shear strain-based algorithm can predict proteoglycan loss in damaged articular cartilage. Biomech Model Mechanobiol 18:753–778. https://doi.org/10.1007/s10237-018-01113-1
11. Eskelinen ASA, Tanska P, Florea C et al (2020) Mechanobiological model for simulation of injured cartilage degradation via proinflammatory cytokines and mechanical stimulus. PLoS Comput Biol 16:1–25. https://doi.org/10.1371/journal.pcbi.1007998
12. Esrafilian A, Stenroth L, Mononen ME et al (2020a) 12 degrees of freedom muscle force driven fibril-reinforced poroviscoelastic finite element model of the knee joint. IEEE Trans Neural Syst Rehabil Eng 29:123–133. https://doi.org/10.1109/tnsre.2020.3037411; Esrafilian A, Stenroth L, Mononen ME, Vartiainen P, Tanska P, Karjalainen PA, Suomalainen JS, Arokoski J, Saxby DJ, Lloyd DG, Korhonen RK (2022) An EMG-assisted muscle-force driven finite element analysis pipeline to investigate joint- and tissue-level mechanical responses in functional activities: towards a rapid assessment toolbox. IEEE Trans Biomed Eng 69(9):2860–2871. https://doi.org/10.1109/TBME.2022.3156018. Epub 2022 Aug 19.PMID: 35239473
13. Esrafilian A, Stenroth L, Mononen ME et al (2020b) EMG-assisted muscle force driven finite element model of the knee joint with fibril-reinforced poroelastic cartilages and menisci. Sci Rep 10:3026. https://doi.org/10.1038/s41598-020-59602-2; Esrafilian A, Stenroth L, Mononen ME, Vartiainen P, Tanska P, Karjalainen PA, Suomalainen JS, Arokoski JPA, Saxby DJ, Lloyd DG, Korhonen RK (2022) Toward tailored rehabilitation by implementation of a novel musculoskeletal finite element analysis pipeline. IEEE Trans Neural Syst Rehabil Eng 30:789–802. https://doi.org/10.1109/TNSRE.2022.3159685. Epub 2022 Mar 31.PMID: 35286263
14. Guilak F, Nims R, Dicks A et al (2018) Osteoarthritis as a disease of the cartilage pericellular matrix. Matrix Biol 71–72:40–50. https://doi.org/10.1016/j.matbio.2018.05.008
15. Henao-Murillo L, Pastrama MI, Ito K, van Donkelaar CC (2019) The relationship between proteoglycan loss, overloading-induced collagen damage, and cyclic loading in articular cartilage. Cartilage 1–12:1501S–1512S. https://doi.org/10.1177/1947603519885005
16. Hosseini S, Wilson W, Ito K, van Donkelaar C (2014) A numerical model to study mechanically induced initiation and progression of damage in articular cartilage. Osteoarthr Cartil 22:95–103. https://doi.org/10.1016/j.joca.2013.10.010
17. Kar S, Smith DW, Gardiner BS et al (2016) Modeling IL-1 induced degradation of articular cartilage. Arch Biochem Biophys 594:37–53. https://doi.org/10.1016/j.abb.2016.02.008
18. Kokkonen HT, Suomalainen JS, Joukainen A et al (2014) In vivo diagnostics of human knee cartilage lesions using delayed CBCT arthrography. J Orthop Res 32:403–412. https://doi.org/10.1002/jor.22521
19. Koli J, Multanen J, Kujala UM et al (2015) Effects of exercise on patellar cartilage in women with mild knee osteoarthritis. Med Sci Sports Exerc 47:1767–1774. https://doi.org/10.1249/MSS.0000000000000629
20. Korhonen RK, Julkunen P, Wilson W, Herzog W (2008) Importance of collagen orientation and depth-dependent fixed charge densities of cartilage on mechanical behavior of chondrocytes. J Biomech Eng 130:021003. https://doi.org/10.1115/1.2898725
21. Kurz B, Jin M, Patwari P et al (2001) Biosynthetic response and mechanical properties of articular cartilage after injurious compression. J Orthop

Res 19:1140–1146. https://doi.org/10.1016/S0736-0266(01)00033-X
22. Li S, Cao J, Caterson B, Hughes CE (2012) Proteoglycan metabolism, cell death and Kashin-Beck disease. Glycoconj J 29:241–248. https://doi.org/10.1007/s10719-012-9421-2
23. Li Y, Frank EH, Wang Y et al (2013) Moderate dynamic compression inhibits pro-catabolic response of cartilage to mechanical injury, tumor necrosis factor-α and interleukin-6, but accentuates degradation above a strain threshold. Osteoarthr Cartil 21:1933–1941. https://doi.org/10.1016/j.joca.2013.08.021
24. Li Y, Wang Y, Chubinskaya S et al (2015) Effects of insulin-like growth factor-1 and dexamethasone on cytokine-challenged cartilage: relevance to post-traumatic osteoarthritis. Osteoarthr Cartil 23:266–274. https://doi.org/10.1016/j.joca.2014.11.006
25. Lu YC, Evans CH, Grodzinsky AJ (2011) Effects of short-term glucocorticoid treatment on changes in cartilage matrix degradation and chondrocyte gene expression induced by mechanical injury and inflammatory cytokines. Arthritis Res Ther 13:R142. https://doi.org/10.1186/ar3456
26. Mäkelä J, Han S, Herzog W, Korhonen R (2015) Very early osteoarthritis changes sensitively fluid flow properties of articular cartilage. J Biomech 48:3369–3376. https://doi.org/10.1016/j.jbiomech.2015.06.010
27. Mäkelä JTA, Rezaeian ZS, Mikkonen S et al (2014) Site-dependent changes in structure and function of lapine articular cartilage 4 weeks after anterior cruciate ligament transection. Osteoarthr Cartil 22:869–878. https://doi.org/10.1016/j.joca.2014.04.010
28. Martel-Pelletier J, McCollum R, DiBattista J et al (1992) The interleukin-1 receptor in normal and osteoarthritic human articular chondrocytes. Identification as the type I receptor and analysis of binding kinetics and biologic function. Arthritis Rheum 35:530–540. https://doi.org/10.1002/art.1780350507
29. Martin JA, McCabe D, Walter M et al (2009) N-acetylcysteine inhibits post-impact chondrocyte death in osteochondral explants. J Bone Jt Surg Am 91:1890–1897. https://doi.org/10.2106/JBJS.H.00545
30. Mononen M, Liukkonen M, Korhonen R (2019) Utilizing atlas-based modeling to predict knee joint cartilage degeneration: data from the osteoarthritis initiative. Ann Biomed Eng 47:813–825. https://doi.org/10.1007/s10439-018-02184-y
31. Mononen M, Tanska P, Isaksson H, Korhonen R (2016) A novel method to simulate the progression of collagen degeneration of cartilage in the knee: data from the osteoarthritis initiative. Sci Rep 6:21415. https://doi.org/10.1038/srep21415
32. Mow VC, Kuei SC, Lai WM, Armstrong CG (1980) Biphasic creep and stress relaxation of articular cartilage in compression: theory and experiments. J Biomech Eng 102:73–84. https://doi.org/10.1115/1.3138202
33. Munukka M, Waller B, Rantalainen T et al (2016) Efficacy of progressive aquatic resistance training for tibiofemoral cartilage in postmenopausal women with mild knee osteoarthritis: a randomised controlled trial. Osteoarthr Cartil 24:1708–1717. https://doi.org/10.1016/j.joca.2016.05.007
34. Myller KAH, Korhonen RK, Töyräs J et al (2019) Computational evaluation of altered biomechanics related to articular cartilage lesions observed in vivo. J Orthop Res 37:1042–1051. https://doi.org/10.1002/jor.24273
35. Nagase H, Kashiwagi M (2003) Aggrecanases and cartilage matrix degradation. Arthritis Res Ther 5:94–103. https://doi.org/10.1186/ar630
36. Ojanen SP, Finnilä MAJ, Mäkelä JTA et al (2020) Anterior cruciate ligament transection of rabbits alters composition, structure and biomechanics of articular cartilage and chondrocyte deformation 2 weeks post-surgery in a site-specific manner. J Biomech 98:109450. https://doi.org/10.1016/j.jbiomech.2019.109450
37. Orozco GA, Eskelinen ASA, Kosonen JP et al (2022) Shear strain and inflammation-induced fixed charge density loss in the knee joint cartilage following ACL injury and reconstruction: a computational study. J Orthop Res 40:1505–1522. https://doi.org/10.1002/jor.25177
38. Orozco GA, Tanska P, Florea C et al (2018) A novel mechanobiological model can predict how physiologically relevant dynamic loading causes proteoglycan loss in mechanically injured articular cartilage. Sci Rep 8:1–16. https://doi.org/10.1038/s41598-018-33759-3
39. Orozco GA et al (2020) Prediction of local fixed charge density loss in cartilage following ACL injury and reconstruction: A computational proof-of-concept study with MRI follow-up. J Orthop Res 39(5):1064–1081. [John Wiley and Sons]
40. Patwari P, Gaschen V, James I et al (2004) Ultrastructural quantification of cell death after injurious compression of bovine calf articular cartilage. Osteoarthr Cartil 12:245–252. https://doi.org/10.1016/j.joca.2003.11.004
41. Pedoia V, Su F, Amano K et al (2017) Analysis of the articular cartilage T1ρ and T2 relaxation times changes after ACL reconstruction in injured and contralateral knees and relationships with bone shape. J Orthop Res 35:707–717. https://doi.org/10.1002/jor.23398
42. Pizzolato C, Reggiani M, Saxby DJ et al (2017) Biofeedback for gait retraining based on real-time estimation of tibiofemoral joint contact forces. IEEE Trans Neural Syst Rehabil Eng 25:1612–1621. https://doi.org/10.1109/TNSRE.2017.2683488
43. Ramdhian-Wihlm R, Le Minor JM, Schmittbuhl M et al (2012) Cone-beam computed tomography arthrography: an innovative modality for the evaluation of wrist ligament and cartilage injuries. Skelet Radiol 41:963–969. https://doi.org/10.1007/s00256-011-1305-1
44. Riad R, Jennane R, Brahim A et al (2018) Texture analysis using complex wavelet decomposition for knee osteoarthritis detection: data from the

osteoarthritis initiative. Comput Electr Eng 68:181–191. https://doi.org/10.1016/j.compeleceng.2018.04.004
45. Sah R, Kim Y, Doong J et al (1989) Biosynthetic response of cartilage explants to dynamic compression. J Orthop Res 7:619–636. https://doi.org/10.1002/jor.1100070502
46. Sauerland K, Raiss R, Steinmeyer J (2003) Proteoglycan metabolism and viability of articular cartilage explants as modulated by the frequency of intermittent loading. Osteoarthr Cartil 11:343–350. https://doi.org/10.1016/S1063-4584(03)00007-4
47. Seedhom BB (2006) Conditioning of cartilage during normal activities is an important factor in the development of osteoarthritis. Rheumatology 45:146–149. https://doi.org/10.1093/rheumatology/kei197
48. Simon BR (1992) Multiphase poroelastic finite element models for soft tissue structures. ASME Appl Mech Rev 45:191–218. https://doi.org/10.1115/1.3121397
49. Smith RL, Carter DR, Schurman DJ (2004) Pressure and shear differentially alter human articular chondrocyte metabolism: a review. Clin Orthop Relat Res 427:S89–S95
50. Son KM, Hong JI, Kim D et al (2020) Absence of pain in subjects with advanced radiographic knee osteoarthritis. BMC Musculoskelet Disord 21:640
51. Stolberg-Stolberg JA, Furman BD, William Garrigues N et al (2013) Effects of cartilage impact with and without fracture on chondrocyte viability and the release of inflammatory markers. J Orthop Res 31:1283–1292. https://doi.org/10.1002/jor.22348
52. Su F, Hilton JF, Nardo L et al (2013) Cartilage morphology and T1ρ and T2 quantification in ACL-reconstructed knees: a 2-year follow-up. Osteoarthr Cartil 21:1058–1067. https://doi.org/10.1016/j.joca.2013.05.010
53. Sui Y, Lee JH, DiMicco MA et al (2009) Mechanical injury potentiates proteoglycan catabolism induced by interleukin-6 with soluble interleukin-6 receptor and tumor necrosis factor α in immature bovine and adult human articular cartilage. Arthritis Rheum 60:2985–2996. https://doi.org/10.1002/art.24857
54. Takahashi K, Goomer RS, Harwood F et al (1999) The effects of hyaluronan on matrix metalloproteinase-3 (MMP-3), interleukin-1β (IL-1β), and tissue inhibitor of metalloproteinase-1 (TIMP- 1) gene expression during the development of osteoarthritis. Osteoarthr Cartil 7:182–190. https://doi.org/10.1053/joca.1998.0207
55. Tanska P, Julkunen P, Korhonen R (2018) A computational algorithm to simulate disorganization of collagen network in injured articular cartilage. Biomech Model Mechanobiol 17:689–699. https://doi.org/10.1007/s10237-017-0986-3
56. Tiulpin A, Klein S, Bierma-Zeinstra SMA et al (2019) Multimodal machine learning-based knee osteoarthritis progression prediction from plain radiographs and clinical data. Sci Rep 9:20038. https://doi.org/10.1038/s41598-019-56527-3
57. Venäläinen M, Mononen M, Salo J et al (2016) Quantitative evaluation of the mechanical risks caused by focal cartilage defects in the knee. Sci Rep 6:37538. https://doi.org/10.1038/srep37538
58. Vincenti M, Brinckerhoff C (2002) Transcriptional regulation of collagenase (MMP-1, MMP-13) genes in arthritis: integration of complex signaling pathways for the recruitment of gene-specific transcription factors. Arthritis Res 4:157–164. https://doi.org/10.1186/ar401
59. Wang K, Kim HA, Felson DT et al (2018) Radiographic knee osteoarthritis and knee pain: cross-sectional study from five different racial/ethnic populations. Sci Rep 8:1–8. https://doi.org/10.1038/s41598-018-19470-3
60. Wilson W, Van Donkelaar CC, Van Rietbergen B, Huiskes R (2005) A fibril-reinforced poroviscoelastic swelling model for articular cartilage. J Biomech 38:1195–1204. https://doi.org/10.1016/j.jbiomech.2004.07.003
61. Zhao R, Dong Z, Wei X et al (2021) Inflammatory factors are crucial for the pathogenesis of post-traumatic osteoarthritis confirmed by a novel porcine model: "idealized" anterior cruciate ligament reconstruction and gait analysis. Int Immunopharmacol 99:107905. https://doi.org/10.1016/j.intimp.2021.107905